Updated NGA-West2 Ground Motion Prediction Equations for Active Tectonic Regions Worldwide

Kenneth W. Campbell[1] and Yousef Bozorgnia[2]

1. Corresponding Author. Vice President, EQECAT, Inc., 1130 NW 161st Place, Beaverton, OR 97006, USA. Email: KWCampbell@eqecat.com

2. Research Fellow, Executive Director, PEER, 325 Davis Hall, University of California, Berkeley, CA 94720, USA. Email: yousef@berkeley.edu

Abstract

We used an expanded PEER NGA-West2 database to develop a new ground motion prediction equation (GMPE) for the average (RotD50) horizontal components of PGA, PGV, and 5%-damped pseudo-absolute acceleration response spectra at 21 periods ranging from 0.01 to 10 s. In addition to those terms included in our now superseded 2008 GMPE, we include a more-detailed hanging-wall model, scaling with hypocentral depth and fault dip, regionally independent geometric attenuation, regionally dependent anelastic attenuation and site conditions, and magnitude-dependent aleatory variability. The NGA-West2 database provides better constraints on both magnitude-scaling and distance-attenuation of small-magnitude earthquakes and anelastic attenuation at large distances, where our 2008 GMPE was known to be biased. We consider our new GMPE to be valid for estimating ground motions from worldwide shallow continental earthquakes in active tectonic regions for magnitudes ranging from 3.3 to 7.5–8.5, depending on source mechanism, and rupture distances ranging from 0–300 km.

Keywords: ground motion prediction equation, GMPE, attenuation relation, active tectonic region

1. INTRODUCTION

The 2012 update of the Australian national seismic hazard maps (Burbidge 2012) uses ground motion prediction equations (GMPEs) from active tectonic regions as one alternative for estimating ground motions in Australia. In fact, Allen (2010, 2012) and Allen et al. (2011) found that the NGA (now NGA-West1) GMPE for active tectonic regions of Chiou and Youngs (2008) was one of the models that compared best over all periods with ground motion data from both Western Australia and SE Australia. Higher weight is given to this model in the more tectonically deformed eastern Australian region than in the more stable region of western Australia. This is consistent with an earlier study by Allen et al. (2005) who found that the GMPE for active tectonic regions of Sadigh et al. (1997) compared well with a stochastic simulation-based model developed for SE Australia. Somerville et al. (2009) also found that their numerical simulation-based GMPE for eastern Australia was very similar to the NGA-West1 GMPEs developed and applied in worldwide tectonically active shallow crustal regions (Power et al. 2008). In this paper, we present an

updated version of the Campbell and Bozorgnia (2008) NGA-West1 GMPE for global tectonically active regions that, based on the conclusions noted above, we suggest is also a candidate for possible use in Australia, especially SE Australia.

The GMPE presented in this paper represents the culmination of a four-year multidisciplinary study sponsored by the Pacific Earthquake Engineering Research Center (PEER) and referred to as the Next Generation Attenuation Phase 2 (NGA-West2) Ground Motion Project (Bozorgnia et al. 2013). This new GMPE supersedes our previous NGA-West1 models for peak ground acceleration (PGA), peak ground velocity (PGV), and 5%-damped linear pseudo-absolute acceleration response spectral ordinates (PSA) at 21 periods ranging from 0.01 to 10 s. Our 2013 and 2008 GMPEs are referred to as CB13 and CB08, respectively, in the remainder of this paper. The CB13 model represents a major update of CB08 made possible by the extensive expansion of the PEER strong motion database and the supporting studies on 1-D ground motion simulation sponsored by the NGA Projects. This paper provides a brief description of the database, functional forms, and analyses that went into the development of CB13, followed by a comparison of CB13 and CB08. Additional documentation is provided in Campbell and Bozorgnia (2013a,b).

2. DATABASE

The ground motion database used in this study is a subset of the PEER NGA-West2 database (Ancheta et al. 2013). The NGA-West2 database includes over 21,000 three-component recordings from worldwide earthquakes with moment magnitudes (**M**) ranging from 3.0 to 7.9. The database includes recordings that for the most part represent free-field site conditions. In order to increase the reliability of our selected database, we applied the same general selection and exclusion criteria that were used to develop CB08. These criteria are listed in Campbell and Bozorgnia (2013a,b). Notable differences from CB08 are the definition of an "aftershock" (aftershocks or what are now called Class 2 events are excluded as before), the inclusion of recordings to distances of 500 km in order to better quantify anelastic attenuation, the inclusion of California earthquakes down to **M** 3.0 in order to better quantify the magnitude and distance scaling of small-to-moderate earthquakes, and the regionalisation of site effects and anelastic attenuation. The application of the above criteria resulted in the selection of a total of 15,521 recordings from 322 earthquakes ($3.0 \leq \mathbf{M} \leq 7.9$). Figure 1 shows the distribution of the recordings with respect to **M** and R_{RUP}.

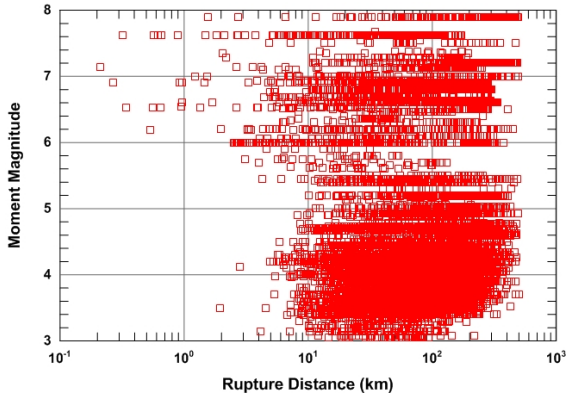

Figure 1. Distribution of recordings with magnitude and distance.

Our selected database can be compared to the 1,561 recordings from 64 earthquakes ($4.3 \leq \mathbf{M} \leq 7.9$) used to develop CB08. The CB13 database includes 7,208 near-source ($R_{RUP} \leq 80$ km) recordings from 282 worldwide earthquakes and 8,313 far-source ($80 < R_{RUP} \leq 500$ km) recordings from 276 earthquakes, where R_{RUP} is closest distance to the rupture plane of the earthquake.

3. GROUND MOTION MODEL

The functional forms for the mathematical terms used in CB13 were developed or confirmed using standard data exploration techniques, including analysis of residuals. Candidate functional forms were developed or selected through numerous iterations to capture the observed trends in the recorded ground motion data. We started with the functional forms in CB08. The hanging-wall term was updated using the hanging-wall model of Donahue and Abrahamson (2013) developed from ground motion simulations. We also included new terms for fault dip and hypocentral depth that were developed from an analysis of residuals. The inclusion of large-distance recordings facilitated the addition of an anelastic attenuation term which, unlike the geometric attenuation term, was found to be regionally dependent. The aleatory standard deviations were modified to be magnitude-dependent in order to accommodate the larger dispersion of the small-magnitude recordings.

The average horizontal component used in CB13 (RotD50) is a simpler version of the horizontal component used in CB08 (GMRotI50). Its merits and comparison with GMRotI50 is given in Boore (2010). The natural logarithm of the RotD50 horizontal components of PGA (g), PGV (cm/s), and PSA (g) is given by the following generalised median ground motion model:

$$\ln(Y) = f_{mag} + f_{dis} + f_{flt} + f_{hng} + f_{site} + f_{sed} + f_{hyp} + f_{dip} + f_{atn} \quad (1)$$

where Y is the ground motion intensity measure of interest and the functions (f-terms) represent the scaling of ground motion with respect to earthquake magnitude, geometric attenuation, style-of-faulting, hanging-wall geometry, shallow site response, shallow and deep basin response, hypocentral depth, fault dip, and anelastic attenuation, respectively. Because of paper length restrictions, the functional forms of these terms cannot be presented. Instead, the reader is referred to Campbell and Bozorgnia (2013a,b).

Consistent with the random-effects regression analysis used to derive the coefficients in the GMPE, the aleatory variability model for ln(Y) has both between-event (inter-event) and within-event (intra-event) components, with standard deviations denoted τ and ϕ, respectively, and a total variance of $\sigma^2 = \tau^2 + \phi^2$. With the addition of small magnitude recordings, both standard deviations were found to be magnitude-dependent. Nonlinear site effects for both τ and ϕ are taken into account, which reduces their values for soft soils and strong shaking. In CB08, only ϕ (previously denoted σ) incorporated nonlinear site effects. The reader is referred to Campbell and Bozorgnia (2013a,b) for additional details.

4. RESULTS

The model coefficients and standard deviations were derived using random-effects regression analysis (Abrahamson and Youngs 1992). f_{atn} accounts for the regional differences in anelastic attenuation for those regions where sufficient data are

available to determine a separate anelastic attenuation coefficient. The base region includes California, Taiwan, the Middle East and similar active tectonic domains, which define an average attenuation region. Other regions include Japan and Italy (JI), which define a relatively higher attenuation region both of which are volcanic, and eastern China (CH), which defines a relatively lower more tectonically stable attenuation region. Unlike anelastic attenuation, we found that the geometric attenuation term, f_{dis}, was regionally independent. f_{site} and f_{sed} account for regional differences in shallow site effects and shallow sediment effects between the U.S. (primarily California) and Japan.

4.1 MODEL VALIDATION

In order to evaluate the validity of our GMPE, we plotted the between-event and within-event residuals against the predictor variables included in the model. Example residual plots of between-event residuals versus **M** and within-event residuals versus R_{RUP} are shown in Figures 2 and 3 for PGA, PGV and PSA at 0.2 s and 1.0 s periods. Additional plots are shown in Campbell and Bozorgnia (2013a,b). In these figures a positive residual indicates underestimation by the model and a negative residual indicates overestimation by the model. The plots shown here and in Campbell and Bozorgnia (2013a,b) indicate that there are no systematic trends or biases in the residuals that would indicate that the model is inconsistent with the data.

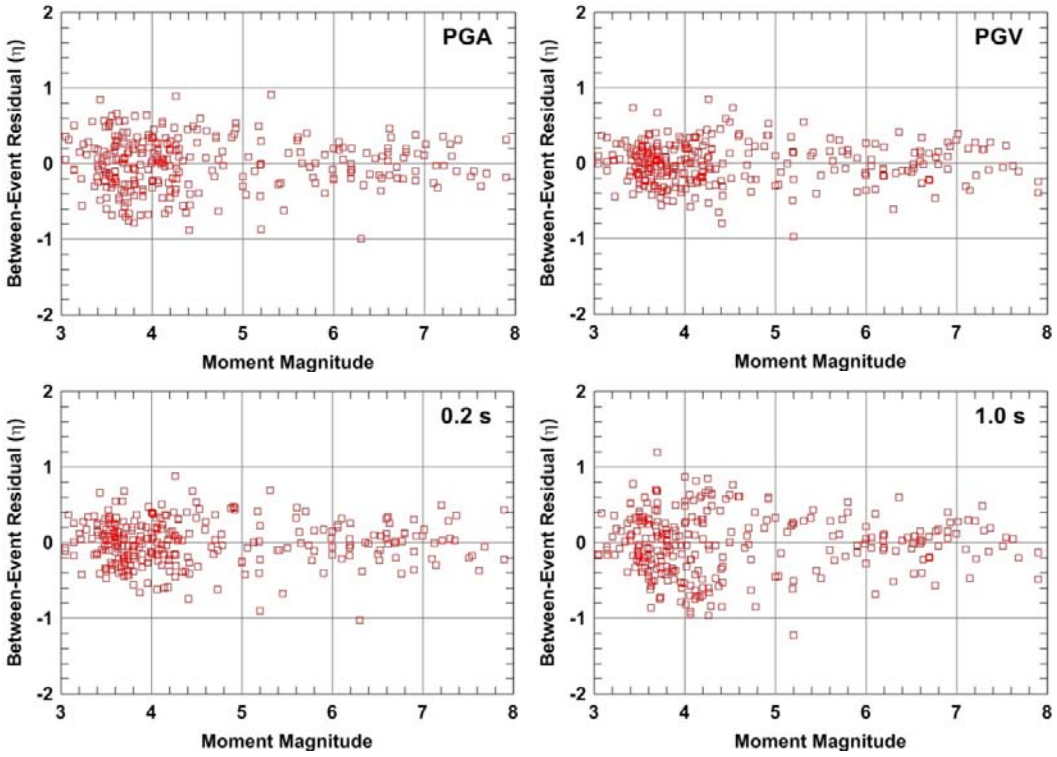

Figure 2. Distribution of between-event residuals with magnitude.

4.2 MODEL EVALUATION

Figure 4 compares how the predicted value of PGA scales with **M** and R_{RUP} between CB08 and CB13 for R_{RUP} = 10 km, V_{S30} = 760 m/s, and a site located on the hanging wall of a 45° dipping reverse fault, where V_{S30} is the time-averaged velocity in the top 30 m of a site. The large difference for **M** 4.5 (left) is due to the previously identified

bias in CB08 ground motion predictions at small magnitudes. The stronger attenuation of CB13 with distance is due to the addition of an anelastic attenuation term. Differences at short distances for **M** 6.5 (right) are due to the revision of the hanging-wall term.

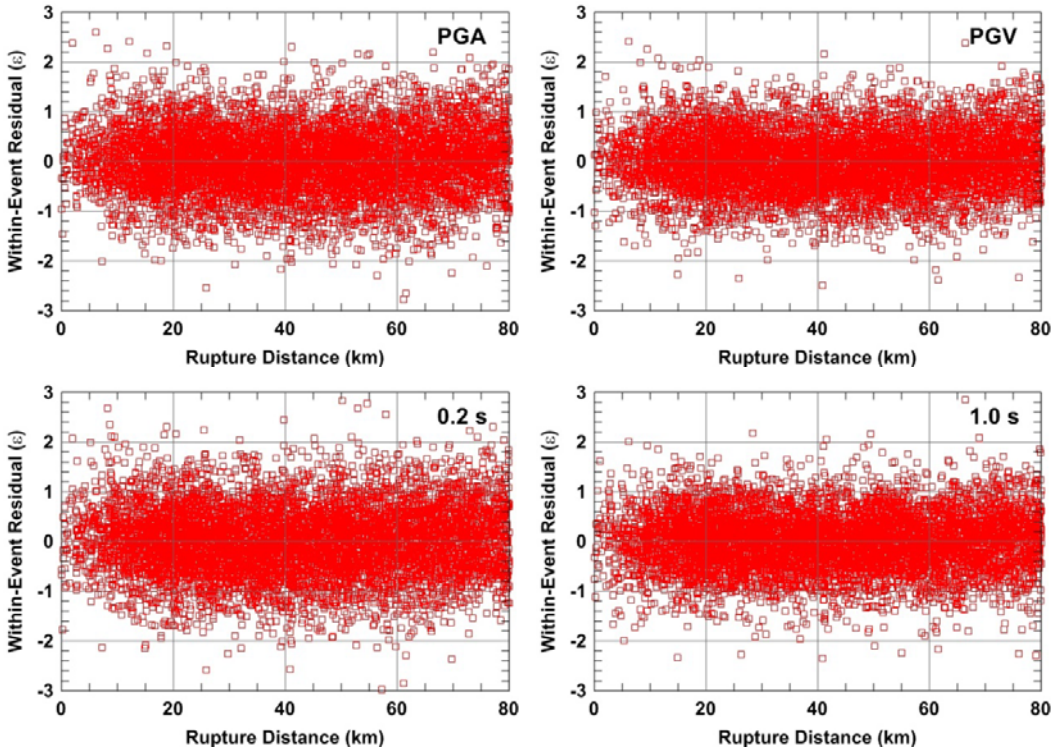

Figure 3. Distribution of within-event residuals with distance.

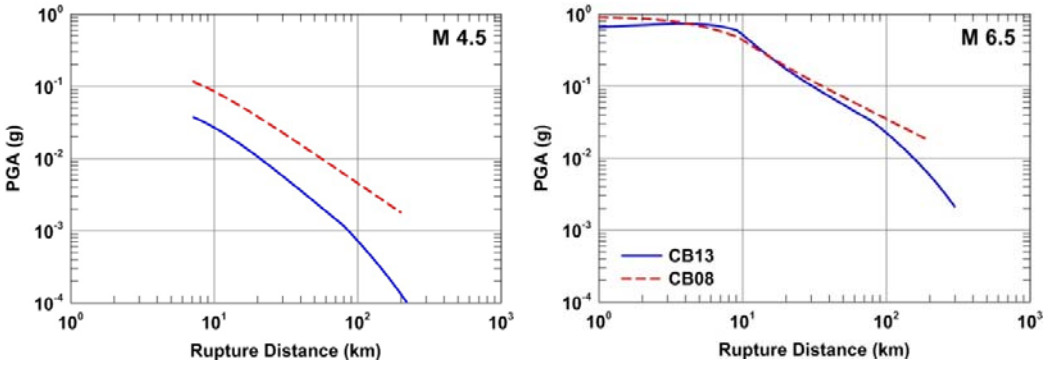

Figure 4. Scaling of PGA with distance for a hanging-wall site on a 45° dipping fault.

Figure 5 shows how PGA (left) and PSA at 1 s period attenuates with distance for **M** 3.5, 4.5, 5.5, 6.5 and 7.5, V_{S30} = 760 m/s, and vertical strike-slip faulting. At short distances, the curves are truncated at the default value of the depth to the top of the rupture plane as explained in Campbell and Bozorgnia (2013a,b). This figure demonstrates the predicted effects of magnitude-dependent geometrical attenuation for R_{RUP} < 80 km, anelastic attenuation for larger distances, and magnitude saturation at large magnitudes and short distances. Figure 6 shows predicted response spectra for **M** 3.5, 4.5, 5.5, 6.5 and 7.5, R_{RUP} = 10 km, and V_{S30} = 760 m/s (left) and how they compare to CB08 (right) for the larger magnitudes where CB08 is most valid. The

biggest difference is at short periods where CB13 predicts larger amplitudes. Additional plots are shown in Campbell and Bozorgnia (2013a,b).

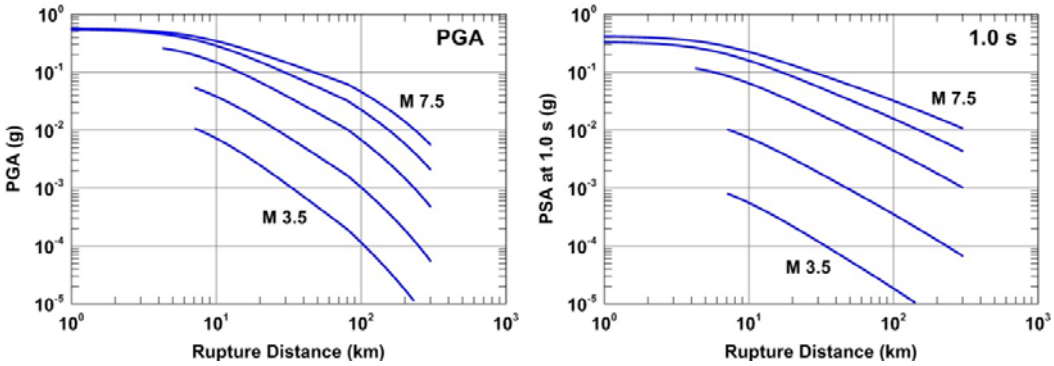

Figure 5. Scaling of PGA and 1-s PSA with distance for a vertical strike-slip fault.

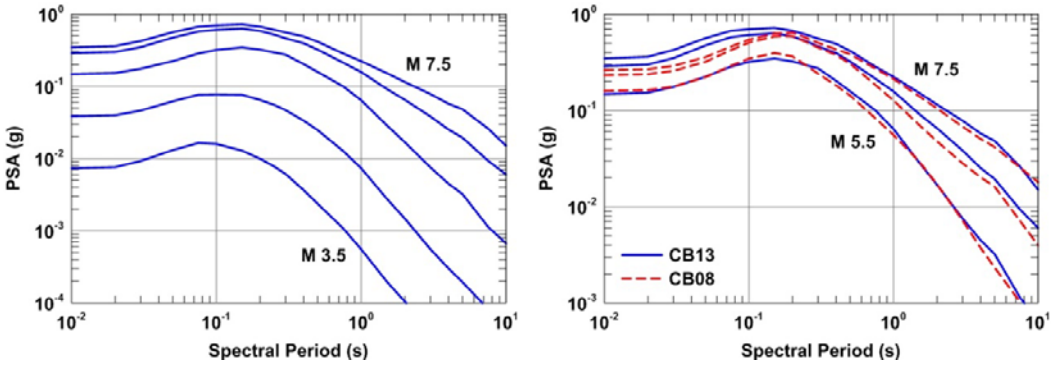

Figure 6. Scaling of response spectra with magnitude for R_{RUP} = 10 km.

Finally, Figure 7 shows how the predicted response spectral shape and amplitude changes with NEHRP site conditions and rock PGA (V_{S30} = 1100 m/s) amplitudes of 0.1*g* (linear response) and 0.5*g* (nonlinear response). Predictions are for **M** 7.5 and values of R_{RUP} commensurate with the designated levels of rock PGA.

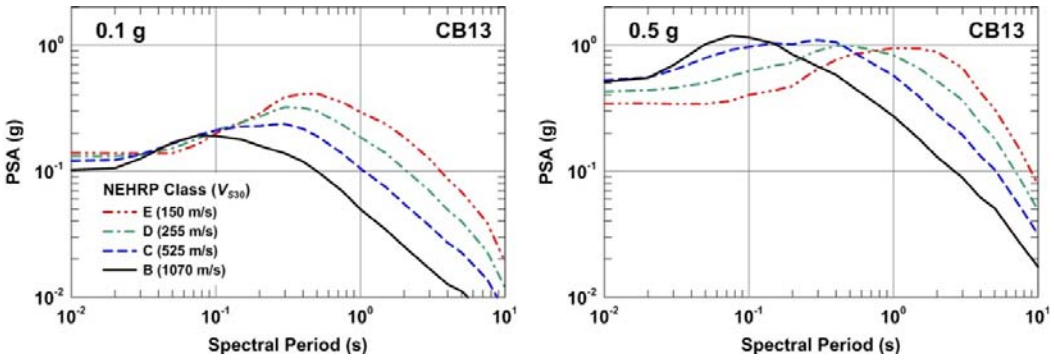

Figure 7. Scaling of response spectra with V_{S30} for **M** 7.5 and R_{RUP} = 10 km.

5. CONCLUSIONS

As a result of the extensive increase in the number of earthquakes and recordings available in the PEER NGA-West2 database, we consider our NGA-West2 model (CB13) to supersede our NGA-West1 model (CB08). CB13 incorporates such

important features and effects as period-dependent magnitude saturation, magnitude-dependent style-of-faulting, magnitude-dependent scaling with hypocentral depth and fault dip, magnitude-dependent but regionally independent geometric attenuation, regionally dependent anelastic attenuation, updated hanging-wall effects, regionally dependent shallow linear and nonlinear site response, regionally dependent shallow sediment effects, and magnitude-dependent nonlinear between-event and within-event aleatory variability.

The comparison of CB13 and CB08 indicates that the impact of our new model on ground motion predictions for **M** > 5.5 and R_{RUP} < 100 km is relatively small, implying that our prediction of near-source moderate-to-large magnitude ground motion is becoming relatively stable. The largest differences between CB13 and CB08 are for hanging-wall effects over the rupture plane, small-magnitude earthquakes, short-period amplitudes at large magnitudes and short distances, and large distances. The modification of the hanging-wall term was the result of a comprehensive study of ground motion simulations sponsored by the NGA-West2 Project. The improvements in small-magnitude and far-source scaling are the direct result of the major effort of PEER to process tens of thousands of recordings of **M** = 3.0–5.5 earthquakes that were recorded by strong motion and broadband networks in California. We believe that this shift in the spectral peak to shorter periods and its associated higher short-period spectral amplitudes as compared to CB08 are due potentially to four changes in our model: (1) an increase in magnitude scaling at short distances and large magnitudes, (2) an increase in the default estimates of hypocentral depth with magnitude, (3) a decrease in the default values of sediment depth with V_{S30}, and (4) a stronger dependence of response spectral shape on site conditions (Campbell and Bozorgnia 2013a,b).

Practical guidance on how to use the model in seismic hazard analysis and engineering applications, especially when some of the parameters in the model are unknown, is given in Campbell and Bozorgnia (2013a,b). A simpler version of the GMPE for use for seismic hazard studies in regions where limited tectonic, geologic, and site information is available will be the topic of a future study.

6. REFERENCES

Abrahamson, N.A. and Youngs, R.R. (1992). A stable algorithm for regression analyses using the random effects model, Bull. Seismol. Soc. Am., Vol. 82, pp. 505-510.

Allen, T., Cummons, P.R., Dhu, T. and Peck, W. (2005). Ground-motion attenuation modelling in Australia; Implications for earthquake hazard and risk, Proc., Australian Earthquake Engineering Society 205 Conference, Albury, New South Wales, Paper No. 41, 8 pp.

Allen, T. (2010). The influence of attenuation in earthquake ground-motion and magnitude estimation: Implications for Australian earthquake hazard, Proc., Australian Earthquake Engineering Society 2010 Conference, Perth, Western Australia, Paper No. 1, 13 pp.

Allen, T., Leonard, M. and Collins, C. (2011). The 2012 Australian seismic hazard map – Catalogue and ground motion prediction equations, Proc., Australian Earthquake Engineering Society 2011 Conference, Barossa Valley, South Australia, Paper No. 4, 153 pp.

Allen, T.I. (2012). Ground-motion prediction equations, in The 2012 Australian Earthquake Hazard Map, Burbidge, D.R. (ed.), Chapt. 5, pp. 44-53.

Ancheta, T.D., Darragh, R.B., Stewart, J.P., Seyhan, E., Silva, W.J., Chiou, B.S.J., Wooddell, K.E., Graves, R.W., Kottke, A.R., Boore, D.M., Kishida, T. and Donahue, J.L. (2013). PEER NGA-West2 Database, PEER Report 2013/03, Pacific Earthquake Engineering Research Center, University of California, Berkeley, CA.

Boore, D.M. (2010). Orientation-independent, nongeometric-mean measures of seismic intensity from two horizontal components of motion, Bull. Seismol. Soc. Am., Vol. 100, pp. 1830-1835.

Bozorgnia, Y. and the NGA-West2 Project Team (2013). Overview of NGA-West2 project, Earthq. Spectra, in press.

Burbidge, D.R. (ed.) (2012). The 2012 Australian earthquake hazard map, Geoscience Australia Record 2012/71.

Campbell, K.W. and Bozorgnia, Y. (2008). NGA ground motion model for the geometric mean horizontal component of PGA, PGV, PGD and 5% damped linear-elastic response spectra for periods ranging from 0.01 and 10.0 s, Earthq. Spectra, Vol. 24, pp. 139-171.

Campbell, K.W. and Bozorgnia, Y. (2013a). NGA-West2 Campbell-Bozorgnia ground motion model for the horizontal components of PGA, PGV, and 5%-Damped elastic pseudo-acceleration response spectra for periods ranging from 0.01 to 10 s, PEER Report 2013/06, Pacific Earthquake Engineering Research Center, University of California, Berkeley, CA.

Campbell, K.W. and Bozorgnia, Y. (2013b). Campbell-Bozorgnia NGA-West2 ground motion model for the average horizontal components of PGA, PGV, and 5%-damped linear acceleration response spectra, Earthq. Spectra, in press.

Donahue, J.L. and Abrahamson, N.A. (2013). Hanging-wall scaling using finite-fault simulations, PEER Report 2013/14, Pacific Earthquake Engineering Research Center, University of California, Berkeley, CA.

Power, M., Chiou, B., Abrahamson, N., Bozorgnia, Y., Shantz, T. and Roblee, C. (2008). An overview of NGA project, Earthq. Spectra, Vol. 24, pp. 3-21.

Sadigh, K., Chang, C.-Y., Egan, J.A., Makdisi, F. and Youngs, R.R. (1997). Attenuation relationships for shallow crustal earthquakes based on California strong motion data, Seismol. Res. Lett., Vol. 68, pp. 180-189.

Somerville, P., Graves, R., Collins, N., Song, S.-G., Ni, S. and Cummins, P. (2009). Source and ground motion models for Australian earthquakes, Proc., Australian Earthquake Engineering Society 2009 Conference, Newcastle, New South Wales, Paper No. 5, 9 pp.